3-30-2007

Suppression of DGAT2 Expression Improves Hepatic Steatosis and Prevents Fat Induced Insulin Resistance

Ameya Kulkarni

Follow this and additional works at: http://elischolar.library.yale.edu/ymtdl

SUPPRESSION OF DGAT2 EXPRESSION IMPROVES HEPATIC STEATOSIS AND PREVENTS FAT INDUCED INSULIN RESISTANCE

A Thesis Submitted to the Yale University School of Medicine in Partial Fulfillment of

the Requirements for the Degree of Doctor of Medicine

By

Ameya Ravindrakumar Kulkarni

2006

ABSTRACT

SUPPRESSION OF DGAT2 EXPRESSION IMPROVES HEPATIC STEATOSIS AND PREVENTS FAT INDUCED INSULIN RESISTANCE.
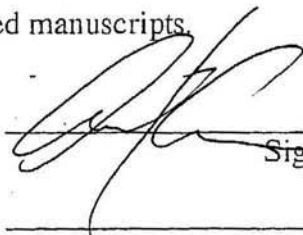
Ameya Kulkarni, Cheol S. Choi,, David Savage, Katsutaro Morino, Varman T. Samuel, Sheene Kim, Amy Wang, John G. Geisler, Sanjay Bhanot, Brett Monia, Xing-Xian Yu, Susanne Neschen, Anthony J. Romaneli, Gerald I. Shulman. Department of Internal Medicine, Yale University School of Medicine, New Haven, CT.

It is well known that metabolites resulting from the accumulation of fat in tissue results in fatty liver, obesity, and insulin resistance. Because triglyceride synthesis is essential for this process, inhibition of the final step of TG synthesis has been considered as a new therapeutic target for hepatosteatosis and insulin resistance. In this study, we investigated the metabolic impact of acyl CoA: diacylglycerol acyltransferase 1 (DGAT1) and 2 (DGAT2) suppression. We used antisense oligonucleotides (ASOs) to reduce the expression of these enzymes in liver and fat in Sprague Dawley rats fed a 27% safflower oil high fat diet (HFD) for 4 weeks. Rats were injected with one of the following: saline, control ASO, DGAT1 ASO or DGAT2 ASO subcutaneously twice a week for 4 weeks. DGAT1 and DGAT2 ASO treatment reduced DGAT1 and DGAT2 mRNA levels in liver by 95% and 57% respectively but only DGAT2 ASO treatment significantly reduced TG content when compared to the saline group. We determined the effects of ASO treatment on insulin action in vivo during a 135 min hyperinsulinemic(4mU/kg/min)-euglycemic clamp. Glucose turnover and uptake were assessed using $[3\text{-}^3H]$glucose infusion and $[1\text{-}^{14}C]$2-deoxyglucose injection during clamps. DGAT2 ASO treated rats were protected from HFD induced insulin resistance as demonstrated by an 80% increase in glucose infusion rate (24.0 ± 0.9 vs. 13.4 ± 1.1 mg/kg/min, $p<0.001$). This was accounted for by significant suppression of hepatic glucose production (82 ± 6 vs. $53\pm11\%$ $p<0.05$) and a 54% increase in insulin-stimulated whole body glucose uptake (25.3 ± 1.1 vs. 16.3 ± 0.7 mg/kg/min, $p<0.001$) when compared to the control ASO group. Insulin-stimulated glucose uptake in skeletal muscle and suppression of plasma free fatty acid levels during the clamp were also significantly increased in DGAT2 ASO treated rats when compared to controls (2DG uptake: 329 ± 31 vs. 263 ± 28 nmol/g/min, $p=0.03$, suppression of FFA: 64 ± 4 vs. $48\pm5\%$, $p=0.015$). Of note, the DGAT2 ASO group showed less weight gain than controls despite the same food consumption over the treatment period. The ratio of weight gain versus food consumption, efficiency of weight gain, was significantly lower in the DGAT2 group when compared to other groups, suggesting an increase in energy expenditure in the DGAT2 ASO group.

In summary, this study demonstrates that the reduction of DGAT2 using an ASO protects against insulin resistance in liver and peripheral tissue.

ACKNOWLEDGEMENTS

TABLE OF CONTENTS

INTRODUCTION

Type 2 Diabetes Mellitus has rapidly become an epidemic in the United States, with the number of people afflicted quickly approaching 17 million[1]. The problem is also growing worldwide, as it is estimated that 250 million people will be affected by the year 2020[5]. Though the primary insult in the pathogenesis of type 2 diabetes is still uncertain, insulin resistance has been implicated as a major contributor to the clinical manifestations of the disease. Several cross-sectional studies have shown insulin resistance in virtually all patients with type 2 diabetes. In addition, prospective studies have demonstrated the presence of insulin resistance up to two decades before the onset of the disease[2,3,4.]

The intracellular events leading to insulin resistance are still relatively unknown. However, the search for the primary defect in this process has been greatly helped by an understanding of the normal insulin signaling cascade in both myocytes and hepatocytes.

In skeletal muscle cells, insulin signaling begins with insulin binding to its receptor and inducing autophosporylation. This in turn activates tyrosine phosporylation of Insulin Receptor Substrate-1 (IRS-1), which activates phosphatidylinositol 3-kinase (PI-3 Kinase). PI-3 Kinase induces an intracellular signaling cascade involving AKT and other intermediates. The final result of this cascade is the translocation of the GLUT 4 receptor—the primary transporter of glucose into skeletal muscle[5]—onto the cellular membrane. In hepatocytes, IRS-2 phosporylation increases PI-3 kinase and AKT-2 activity. This in turn is thought to activate Glycogen Synthase Kinase 3

(GSK3), resulting in an increase in glycogen synthesis—the primary insulin-mediated activity in the liver[5,20].

Further study of this cascade has implicated the elevation of intracellular lipids as a major contributor to the onset of insulin resistance in muscle and liver. A clear correlation between the accumulation of lipids in the liver and skeletal muscle and the development of insulin resistance has been repeatedly reported[6,7,8,9]. Several studies from Dr. Shulman's group and others have suggested that increasing intracellular fatty acid metabolites activate a serine/threonine kinase cascade (possibly initiated by PKC-θ in rodent muscle[10]) and subsequent activation of other serine kinases such as IKK-β[11,12] and JNK-1[13] lead to phosporylation of serine sites on IRS-1, interfere with insulin stimulation of PI3K and result in insulin resistance[5,14]. A similar process has been suggested in liver, initiated by PKC-ε and mediated by tyrosine phosporylation of IRS-2[35].

Triglycerides, as the major storage molecules for lipid in cells, are a primary source of intracellular fatty acid metabolites. Diacylglycerol acyl transferase (DGAT) catalyzes the final step in triglyceride synthesis by using diacylglycerol and acyl-coenzyme A (acylCoA) (Figure 1). DGAT exists in two primary isoforms: DGAT1 and DGAT2[15]. Although these isoforms are encoded by two separate gene families[15], both enzymes are ubiquitously expressed in tissues that are active in TG synthesis—primarily the liver, adipose tissue, the intestinal epithelium, and epidermis. DGAT1 knockout mice have approximately 50% less TG in tissues[16,17] and are protected from obesity and diet induced insulin resistance through a mechanism involving increased energy expenditure, partially attributable to increased physical activity[16,17]. Study of

DGAT2 has been much more difficult, primarily because homozygous knockout of DGAT2 results in neonatal death due to severe lipopenia and impaired skin barrier function[18].

Comparative study of the two isoforms revealed vastly different enzymes. Genetic analysis showed little genetic homology between DGAT1 and 2, suggesting they came from different gene families[15]. Other studies showed that suppression of one isoform did not result in a compensatory increase in the other[17,18]. Combined with the fact that the highest levels of expression of DGAT1 are in small intestine and white adipose tissue, while DGAT2 is primarily expressed in liver and white adipose tissue[15], these data strongly suggest that the two enzymes play different roles in TG metabolism. Moreover, the extreme reduction in TG (approximately 90% in DGAT2 KO carcass) suggests DGAT2 is more important in triglyceride synthesis than DGAT1. However, no study to date has been able to examine the *in vivo* role of DGAT2 in triglyceride synthesis or the resulting effects on insulin resistance.

To study the role that DGAT1 and DGAT2 play in triglyceride synthesis *in vivo*, we used antisense oligonucleotides (ASOs) to induce a deficiency in DGAT1 and DGAT2 expression in the setting of rats receiving fat enriched diets. Because ASOs are active in liver and adipose tissue but not in skeletal muscle[19], this study provides a unique model to study the effect of the isolated reduction of DGAT expression in liver and adipose tissue. Additionally, it allows an opportunity to study the effect of pharmacologic reduction of triglyceride synthesis on fat induced insulin resistance.

AIMS

1) To characterize the effect of individual suppression of DGAT1 and DGAT2 on hepatic steatosis under high fat feeding conditions.

HYPOTHESIS: Suppression of DGAT1 and DGAT2 will reduce hepatic steatosis in rats fed a high fat diet.

2) To characterize the effect of individual suppression of DGAT1 and DGAT2 on insulin mediated activity in liver and skeletal muscle under high fat feeding conditions

HYPOTHESIS: Both DGAT1 and DGAT2 suppression will protect high fat fed rats from developing hepatic insulin resistance.

METHODS

Note: All experimental protocols were completed by Ameya Kulkarni and Dr. Cheol Soo Choi unless otherwise stated.

Animal Care and Treatments: Healthy male Sprague-Dawley (SD) rats weighing 200-225 g were obtained from Charles River Laboratories (Wilmington, MA) and acclimated for four days after arrival and before initiation of the experiment. Rats were housed individually and maintained on a 12:12 hour light dark cycle (lights on at 6:30 AM) with free access to food and water. Rats received either regular rodent chow (RC: 60 % carbohydrate (CHO)/ 10 % fat/ 30% protein) or a high fat diet (HFD: 26 % CHO/ 59 % fat/ 30 % protein). Safflower oil was the major constituent of the high fat diet (Dyets Inc., Bethlehem, PA). We have previously shown that this diet produces hepatic steatosis and hepatic insulin resistance within 3 days[20]. Thus, intraperitoneal ASO therapy was initiated 3 days after commencing the high fat diet. All ASOs (control, DGAT1 and DGAT2) were prepared in normal saline, and the solutions were sterilized through a 0.2 μm filter. To suppress expression of the targeted gene, rats were dosed with ASO solutions or saline twice per week via intraperitoneal injection at a dose of 50-75mg/kg/week for 4 weeks. This study involved 6 treatment groups: Saline with regular chow (n=7), Saline with high fat diet (HFD) (n=7), DGAT1/HFD (n=11, ASO 50 mg/Kg/week), DGAT2/HFD (n=9, ASO 75mg/Kg/week) and two control/HFD groups(scrambled ASO 50 or 75mg, n=9 and 5, respectively). During the treatment period, body weight and food intake were

measured twice weekly. All procedures were approved by The Yale Animal Care and Use Committee.

Selection of Rat DGAT ASOs: ASOs were selected and produced by Isis Pharmaceuticals in Carlsbad, California. To identify rat DGAT 1 and 2 ASO inhibitors, rapid throughput screens were performed *in vitro*[21]. In brief, eighty ASOs were designed to the rat DGAT1 and 2 mRNAs sequences and initial screens identified several potent and specific ASOs, all of which targeted a binding site within the coding region of the DGAT1 and 2 mRNAs. After extensive dose-response characterization of the most potent ASOs from the screen, two lead ASOs, ISIS-327822 and ISIS-369235 for DGAT1 and 2 respectively, were chosen. The control ASO, ISIS-141923, containing the sequence: 5'-CCTTCCCTGAAGGTTCCTCC-3', did not have perfect complementarity to any known gene in public databases. These ASOs contained a phosphoorthioate backbone, and in addition, the first and last five bases had a 2'-O-(2-methoxy)-ethyl(2'-MOE) modification. This chimeric design has been shown to provide both increased nuclease resistance and mRNA affinity, while maintaining the robust RNase H terminating mechanism utilized by these types of ASOs[22]. These benefits result in an attractive *in vivo* pharmacological and toxicological profile for 2'-MOE chimeric ASOs.

Experimental Protocols:

Two separate studies were performed after an overnight fast (food was removed at 5:00 pm on the day before the experiment, and experiments were started at

approximately 9:00 am.

Study 1: Hyperinsulinemic-Euglycemic Clamp

After the four week treatment period described above, hyperinsulinemic euglycemic

clamp studies were performed to measure peripheral and hepatic insulin sensitivities.

Seven days prior to the clamp studies, Dr. Jianying Dong (rodent surgeon for Dr.

Gerald Shulman) placed indwelling catheters into the right internal jugular vein

extending to the right atrium, and the left carotid artery extending to the aortic arch.

After the seven day waiting period and an overnight fast, $[3-^3H]$-glucose (HPLC

purified; Perkin Elmer, Boston, MA USA) was infused at a rate of 0.15 µCi/min for 2

hours to assess basal glucose turnover. Following the basal period, the

hyperinsulinemic euglycemic clamp was conducted for 135 min with a

primed/continuous infusion of human insulin (40 mU/kg prime, 4 mU/kg/min

infusion) (Novo Nordisk, Princeton, NJ) and a variable infusion of 20% dextrose to

maintain euglycemia (~100 mg/dl). $[3-^3H]$-glucose was infused at a rate of 0.4

µCi/min throughout the clamps to estimate insulin-stimulated whole body glucose

fluxes, and 25 uCi of 2-deoxy-D-$[1-^{14}C]$glucose (DOG; Perkin Elmer, Boston, MA

USA) was injected as bolus at the 75th minute of the clamp to estimate the rate of

insulin-stimulated tissue glucose uptake[23]. Blood samples for the measurement of

plasma ^3H and/or ^{14}C activities (60 µl) were taken at the end of basal period and

every 10 min during the last 45 min of the clamp period. Additional blood samples

(20 ~ 60µl) were taken at 0, 70 and 135min for the determination of plasma free fatty

acids and insulin concentrations. At the end of the clamp, rats were anesthetized with

sodium pentobarbital injection (150mg/kg) and all tissues were taken within 4 min, frozen immediately using liquid N_2-cooled aluminum tongs, and stored at $-80°C$ for subsequent analysis.

Study 2: Temporal Analysis

To study the metabolic effects of DGAT2 suppression over time, groups of rats receiving either high dose negative control ASO (75 mg/kg/week) or DGAT2 (75 mg/kg/week) were treated for either 4 (n=8 and 8), 8 (n=8 and 8), 14 (n=8 and 8) or 28 (n=6 and 7) days. In addition, rats receiving saline/RC (n=5), saline/HFD (n=5) or low dose negative control (50 mg/kg/week) (n=6) were treated for 28 days. Finally, one group was studied after a 3 day high fat diet with no ASO treatment (n=8).

After the respective treatment periods and an overnight fast, rats were anesthetized using inhaled isoflorane. Soleus, gastrocnemius, tibalis anterior, quadriceps, and liver were collected using liquid N_2-cooled aluminum tongs, and stored at $-80°C$ for subsequent analysis. Liver and gastrocnemius were homogenized and triglycerides, diacylglycerols, and fatty acyl CoAs were measured as described below. mRNA was also isolated and quantified as described below. Plasma was collected from the portal vein as used for liver function tests and lipid profiles, as well as to measure insulin, leptin, adiponectin, and resistin.

Biochemical Analysis and Calculations: Plasma glucose was analyzed during the clamps using 10 µl plasma by a glucose oxidase method on a Beckman glucose

analyzer II (Beckman, Fullerton, CA). Plasma insulin was measured by Aida Groszman at the Yale Radioimmunoassay Core Laboratories using radioimmunoassay kit from Linco Research (St. Charles, MO). Plasma Free Fatty Acid was determined using an acyl-CoA oxidase based colorimetric kit (Wako Pure Chemical Industries, Osaka, Japan). For the determination of plasma ^{3}H-glucose and ^{14}C-2-DG, plasma was deproteinized with $ZnSO_4$ and $Ba(OH)_2$, dried to remove ^3H_2O, resuspended in water, and counted in scintillation fluid (Ultima Gold, Perkin Elmer, Boston MA) on a Beckman scintillation counter. Rates of basal and insulin-stimulated whole-body glucose turnover were determined as the ratio of the [3-^{3}H]-glucose infusion rate (disintegrations per minute [dpm] per minute) to the specific activity of plasma glucose (dpms per mg) at the end of basal period and during the final 30 min of the clamp experiment, respectively. Hepatic glucose output (HGO) was determined by subtracting the glucose infusion rate from the total glucose appearance. The plasma concentration of ^3H_2O was determined by the difference between ^{3}H counts without and with drying and whole body glycolysis was calculated from the rate of increase in plasma ^3H_2O concentration, determined by linear regression of the measurements at 100, 105, 115, 125, and 135 min[23]. Whole body glycogen plus lipid synthesis was estimated by subtracting whole body glycolysis from whole body glucose uptake[24]. Glucose uptake and glycogen synthesis in individual muscles were calculated from muscle ^{14}C-2-DG-6-P content and ^{3}H incorporation to muscle glycogen, as previously described[23]. For the determination of muscle ^{14}C-2-DG-6-phosphate (2-DG-6-P) content, muscle samples were homogenized, and the supernatants were subjected to an ion-exchange column to separate 2-DG-6-P from 2-

analyzer II (Beckman, Fullerton, CA). Plasma insulin was measured by Aida Groszman at the Yale Radioimmunoassay Core Laboratories using radioimmunoassay kit from Linco Research (St. Charles, MO). Plasma Free Fatty Acid was determined using an acyl-CoA oxidase based colorimetric kit (Wako Pure Chemical Industries, Osaka, Japan). For the determination of plasma ^{3}H-glucose and ^{14}C-2-DG, plasma was deproteinized with $ZnSO_4$ and $Ba(OH)_2$, dried to remove ^3H_2O, resuspended in water, and counted in scintillation fluid (Ultima Gold, Perkin Elmer, Boston MA) on a Beckman scintillation counter. Rates of basal and insulin-stimulated whole-body glucose turnover were determined as the ratio of the [3-^{3}H]-glucose infusion rate (disintegrations per minute [dpm] per minute) to the specific activity of plasma glucose (dpms per mg) at the end of basal period and during the final 30 min of the clamp experiment, respectively. Hepatic glucose output (HGO) was determined by subtracting the glucose infusion rate from the total glucose appearance. The plasma concentration of ^3H_2O was determined by the difference between ^{3}H counts without and with drying and whole body glycolysis was calculated from the rate of increase in plasma ^3H_2O concentration, determined by linear regression of the measurements at 100, 105, 115, 125, and 135 min[23]. Whole body glycogen plus lipid synthesis was estimated by subtracting whole body glycolysis from whole body glucose uptake[24]. Glucose uptake and glycogen synthesis in individual muscles were calculated from muscle ^{14}C-2-DG-6-P content and ^{3}H incorporation to muscle glycogen, as previously described[23]. For the determination of muscle ^{14}C-2-DG-6-phosphate (2-DG-6-P) content, muscle samples were homogenized, and the supernatants were subjected to an ion-exchange column to separate 2-DG-6-P from 2-

DG as previously described[25]. The radioactivity of ^3H in muscle glycogen was determined by digesting muscle samples in KOH and precipitating glycogen with EtOH as previously described[24].

Insulin Signaling

After a four week ASO treatment period (75 mg/kg/week), these rats underwent a 100 uU regular insulin bolus injection and tissues were harvested *in-situ* exactly 15 min after insulin stimulation. Liver samples harvested *in-situ* in fasting conditions (basal) were used to assess IR, and IRS-2 tyrosine phosphorylation, (n=11) IRS-1 and IRS-2 associated PI3 kinase activity (n=12), Akt2 activity (n=13). Soleus muscles were used for IR, and IRS-1 tyrosine phosphorylation, (n=11) IRS-1 associated PI3 kinase activity (n=12), Akt1 activity (n=13). Primary antibodies used for these experiments were rabbit polyclonal IgG obtained from Upstate (Charlottesville, VA). For assessment of tyrosine phosphorylation, after the membrane was blotted with anti-phosphotyrosine antibody, it was stripped and reblotted with the same antibody used for immunoprecipitation to assess any differences in total protein (i.e. IR, IRS1 or IRS2) present. Antibody and immunoprecipitation experiments were carried out by Dr. Xian Chung.

Tissue Lipid Measurement: The following experiments were completed by Dr. Gary Cline. After purification, fatty acyl-CoA fractions were dissolved in methanol/H_2O (1:1, v/v) and subjected to LC/MS/MS analysis[26,27]. A turbo ionspray source was interfaced with an API 3000 tandem mass spectrometer (Applied Biosystems, Foster City, CA) in conjunction with two Perkin Elmer 200 Series micro pumps and a 200

Series autosampler (Perkin Elmer, Norwalk, CT). The transition pairs [M-2H]2-:[M-H-80]- (Q1 and Q3) were monitored in negative MRM mode for each fatty acyl-CoA species. Total fatty acyl-CoA content is expressed as the sum of individual species. An aliquot of the organic phase was retained for measurement of diacylglycerol content. This was passed over preconditioned columns (Waters Sep-Pak Cartridge WAT020845, Milford, Massachusetts) to purify the DAG component. Using mass spectrometry the transition pairs [M+H-18]+: fatty acids from DAG (Q1 and Q3) were monitored in + MRM mode for each DAG metabolite. Total DAG content is expressed as the sum of individual species. Tissue triglyceride was extracted using the method of Bligh and Dyer[26] and measured using a DCL Triglyceride Reagent (Diagnostic Chemicals Limited, P.E.I. Canada).

Determination of Triglyceride Synthesis and Fatty Acid Oxidation in Transfected Rat Hepatocytes In Vitro

The following experiments were completed by collaborators at Isis Pharmaceuticals in Carlsbad California.

Trigylceride synthesis in transfected rat hepatocytes was determined by measuring the incorporation of radiolabeled glycerol into triglycerides[18]. After a 24 hour recovery, transfected cells cultured into 60-mm plates were switched to 1 ml of high glucose DMEM medium containing 10% FBS, 0.5% BSA and 10 uCi of [³H]glycerol with or without addition of 0.5 mM oleate and cultured overnight. The cells were then harvested. One fraction of the harvested cells were used for RNA extraction and gene expression analysis hexane/isopropanol (3:2 in volume) mixture. The extracted lipids

were separated by TLC. The amount of incorporated [³H]glycerol into triglyceride was determined by liquid scintillation counting. Fatty acid oxidation in the transfected hepatocytes were determined by measuring the oxidation of [¹⁴C]oleate into acid soluble products and CO_2[28]. Briefly, hepatocytes cultured in 25-cm^2 flasks were washed with PBS once and incubated with 2 ml low glucose DMEM plus 0.25% BSA and 0.25 uCi of [¹⁴C]oleic acid (Amersham Biosciences). The flasks were capped with a rubber stopper and gassed with O_2-CO_2 (95%-5%). After 3 h incubation, 1 ml of medium was mixed with 100 ul of 10% BSA and then with 100 ul of 60% $HClO_4$. After centrifugation, 1 ml of the supernatant was counted to determine the levels of soluble ¹⁴C-products. Radiolabeled CO_2 was trapped in a well contained 50 ul of 35% NaOH and directly determined by liquid scintillation counting.

Total RNA Preparation and Real-time Quantitative RT-PCR Analysis

The following experiments were completed by Ameya Kulkarni with significant assistance from Dr. David Savage and Amy Wang.

Total RNA was extracted from harvested hepatocytes or tissues using total RNA isolation reagent (#BL-10500, Biotecx Laboratories Inc, Houston TX) according to manufacturer's instructions. Real-time quantitative RT-PCR was performed using custom-made RT-PCR enzymes and reagents kit (Invitrogen Life Technology Inc, Carlsbad, CA) and ABI Prism 7700 Sequence Detector (PE Applied Biosciences, Foster City, CA). Primers and probes for analysis of the expression of different genes were designed using Primer Express Software (PE Applied Biosciences, Foster City, CA).

were separated by TLC. The amount of incorporated [3H]glycerol into triglyceride was determined by liquid scintillation counting. Fatty acid oxidation in the transfected hepatocytes were determined by measuring the oxidation of [14C]oleate into acid soluble products and CO_2[28]. Briefly, hepatocytes cultured in 25-cm^2 flasks were washed with PBS once and incubated with 2 ml low glucose DMEM plus 0.25% BSA and 0.25 uCi of [14C]oleic acid (Amersham Biosciences). The flasks were capped with a rubber stopper and gassed with O_2-CO_2 (95%-5%). After 3 h incubation, 1 ml of medium was mixed with 100 ul of 10% BSA and then with 100 ul of 60% $HClO_4$. After centrifugation, 1 ml of the supernatant was counted to determine the levels of soluble ^{14}C-products. Radiolabeled CO_2 was trapped in a well contained 50 ul of 35% NaOH and directly determined by liquid scintillation counting.

Total RNA Preparation and Real-time Quantitative RT-PCR Analysis

The following experiments were completed by Ameya Kulkarni with significant assistance from Dr. David Savage and Amy Wang.

Total RNA was extracted from harvested hepatocytes or tissues using total RNA isolation reagent (#BL-10500, Biotecx Laboratories Inc, Houston TX) according to manufacturer's instructions. Real-time quantitative RT-PCR was performed using custom-made RT-PCR enzymes and reagents kit (Invitrogen Life Technology Inc, Carlsbad, CA) and ABI Prism 7700 Sequence Detector (PE Applied Biosciences, Foster City, CA). Primers and probes for analysis of the expression of different genes were designed using Primer Express Software (PE Applied Biosciences, Foster City, CA).

For the analysis, 100 ng of total RNA was used. Each RNA sample was run in duplicate and the mean value was used to calculate the gene expression level.

Fat Absorption

For the following experiments, the rats were treated and stool collected by Ameya Kulkarni. Stool was then sent to Ron Jandacek for fat absorption analysis.

To measure intestinal fat absorption in ASO treated rats, three groups of rats were treated with either Saline (n=5), negative control ASO (n=5) or DGAT2 (n=5) under high fat feeding conditions as described above. During the third week of the treatment period, fat absorption was measured by placing a sucrose polybehenate marker in a safflower oil diet and measuring the percent discarded in collected stool samples[29].

Histologic Analysis.

Liver and epididymal fat were fixed in 10% buffered formalin and embedded in paraffin wax. Multiple adjacent 4-um sections were cut and amounted on glass slides. After dehydration, the sections were stained with hematoxylin and eosin. Images of the histological sections were analyzed by Isis Pharmaceuticals.

Statistical Analysis

Data are expressed as means ± S.E.M. The significance of the differences in mean values among different treatment groups were evaluated using the one way-ANOVA,

followed by *ad hoc* analysis using the (Duncane test). P<0.05 was considered statistically significant.

RESULTS

Consistency of High and Low Dose Control Groups

Weight gain and food intake were similar in all groups except the DGAT2 group, which showed a significantly lower weight gain over the treatment period (Figure 3). As there was no significant difference in weight gain, tissue TG content, lipid profile, hepatic or peripheral insulin sensitivities between the low- and high-dose negative control groups, the data was combined into one negative control ASO group.

Effect of ASO on DGAT 1 and 2 Expression in Liver, White Adipose Tissue, and Skeletal Muscle

Antisense Oligonucleotide therapy reduced gene expression of DGAT1 and 2 by 95% and 57% in liver when compared to scrambled ASO controls. Of note, there was no reduction in gene expression in skeletal muscle. In results consistent with previous data[17,18], DGAT1 and 2 expression did not increase to compensate for deficiency of the other enzyme (Figure 2). There was no evidence of hepatotoxicity, as assessed by serum transaminase concentrations and no variations in food intake between the groups.

Effect of Reduced DGAT 1 and 2 Expression on Food Consumption and Weight Gain

Although food consumption was consistent across all treatment groups (Figure 3), final weights were significantly lower in the DGAT 2 treated animals (374 ± 7.6 vs. 415 ± 9.4, 412 ± 6.0, 404 ± 7.6 and 418 ± 9.1 g for DGAT2 vs Saline/RC, Saline/HFD,

Scrambled/HFD and DGAT1; p<0.05) (Figure 3) Weight gain efficiency, the ratio of weight gain to food consumption, was significantly lower in DGAT2 group(0.26 ± 0.02 vs. 0.31 ± 0.02, 0.30 ± 0.01 and 0.33 ± 0.01 for DGAT2 vs Saline/HFD, Control/HFD and DGAT1, p<0.05) strongly suggesting that the reduced weight gain in the DGAT2 ASO group was metabolic and not secondary to reduced appetite.

Further evidence for a metabolic cause of reduced weight gain in the DGAT 2 treatment group was provided by specific study of intestinal fat absorption by SBP[29]. This experiment revealed no difference in fat absorption between rats treated with the DGAT2 ASO and controls.

Reduction of DGAT2 Gene Expression Reduced Hepatic Triglyceride Content and Improved Plasma Lipid Levels.

Histologic examination (Figure 4) and analysis of liver triglyceride content (9.2 ± 1.1 vs. 20.1 ± 1.5, 15.9 ± 1.4 and 17.0 ± 2.4 mg/g wet liver for DGAT2 vs Saline/HFD, Control/HFD and DGAT1; p<0.05) demonstrated significant improvement in hepatic steatosis in DGAT2 ASO treated rats when compared to controls (Figure 5). There was, however, no significant change in muscle triglyceride content. DGAT2 treatment also improved blood lipid levels, with plasma triglyceride levels 25% lower than scrambled ASO controls (26.2 ± 1.1 vs 35.2 ± 2.4 mg/dl in scrambled; p<0.01).

Reduction of DGAT2 Gene Expression Improved Hepatic and Peripheral Insulin Sensitivities.

The impact of treatment with the DGAT ASO on peripheral and hepatic insulin action was examined with 135 min hyperinsulinemic euglycemic clamps in male SD rats following 4 weeks of treatment with antisense oligonucleotides. Overnight fasted plasma glucose concentrations did not differ among the groups. During the clamp, the plasma insulin concentration was elevated to approximately 600pM, while the plasma glucose concentration was clamped at approximately 5.6 mM in all groups. The glucose infusion rate (GINF) required to maintain euglycemia achieved steady state within 90 min and as a result, all insulin sensitivity indices were calculated after this point. DGAT2 treatment increased whole body insulin response, as reflected by a significantly higher GINF (24.0 ± 0.9 vs. 16.7 ± 1.2, 11.7 ± 1.0, 14.0 ± 0.9 and 13.1 ± 1.7 mg/kg/min for DGAT2 vs Saline/RC, Saline/HFD, Control/HFD and DGAT1; $p < 0.05$) (Figure 6A).

To discern the individual contributions of liver and peripheral tissue to increased insulin response, insulin action on liver and peripheral tissue were measured separately using radioisotope labeled glucose infused during the clamp. While basal hepatic glucose production was similar in all groups, insulin stimulated suppression of hepatic glucose production, a marker of hepatic insulin sensitivity, was significantly increased in the DGAT2 treatment group when compared to controls (82.1 ± 5.5 vs. 48.5 ± 1.5, 50.4 ± 9.5 and 47.5 ± 9.2 % for DGAT2 vs Saline/HFD, Control/HFD and DGAT1; $p < 0.05$) (Figure 6B).

Moreover, DGAT2 ASO treatment increased insulin stimulated whole body glucose uptake and glycogen synthesis rates by 47% and 71% when compared to controls (Figure 6C). This increase in insulin stimulated glucose uptake was predominantly accounted for by a 35% and 230% increase in insulin stimulated glucose uptake in skeletal muscle (Figure 6D) and white adipose tissue (Figure 6E), suggesting a significant improvement in peripheral insulin sensitivity.

The DGAT2 ASO treatment group also demonstrated significantly lower free fatty acid (FFA) levels during the clamp period as well as a 64% reduction of FFA under insulin stimulation (Figure 7), implying an improvement in insulin sensitivity towards suppression of lipolysis from adipose tissue as well.

Of note, DGAT1 suppression did not result in any improvement in hepatic or peripheral insulin sensitivity.

Reduction of DGAT2 Reduced Intracellular Levels of Diacylglycerol

Levels of diacylglycerol and long chain acyl CoA were examined in the hepatocytes of rats treated with either scrambled or DGAT2 ASOs for four weeks under high fat feeding conditions. Although there was no significant difference in long chain acyl CoAs between the two groups(80.2+8.6 vs 82.8+13.3), diacylglycerol levels were significantly lower in the DGAT2 deficient animals (925 + 102 vs 470 + 84, p=0.006) (Figure 8).

DISCUSSION

This study demonstrated that liver and adipose tissue specific inhibition of DGAT2 via ASO results in reduced weight gain, less hepatic steatosis and improved hepatic and peripheral insulin sensitivity in rats fed a high fat diet. Previous studies examining the effects of DGAT2 deficiency used a whole body knockout model, which resulted in severe lipopenia, excessively thin skin and early neonatal death secondary to dehydration[15]. Because the ASO in this study specifically targeted liver and adipose tissue[19], there was no lipopenia in the peripheral tissue or epidermis and thus no peripheral toxicity occurred from DGAT2 deficiency. In addition, the results of this study showed no differences in intestinal fat absorption or food consumption in DGAT2 deficient animals versus controls, and no hepatotoxicity secondary to treatment. This strongly supports the idea that the mechanisms behind the improvements in weight, hepatic fat, and insulin sensitivity are metabolic. Interestingly, despite the liver and adipose specific effect of the ASO, this study did demonstrate some improvement in peripheral insulin resistance, specifically in skeletal muscle. There are several potential explanations for this phenomenon, including an improvement in the general metabolic state of treated animals or a previously unknown muscle specific effect of the ASO. Specific examination of the fatty acid metabolites in muscle is currently being done to determine the causes of this interesting occurrence.

In another important finding in the current study, liver and adipose specific deficiency of DGAT1 did not result in any improvement in insulin sensitivity or hepatic steatosis. This is in stark contrast to previous studies involving whole body deficiency of

DGAT1, which resulted in a significantly improved insulin sensitivity profile[16,17].

Other studies have demonstrated increased activity in mice deficient in DGAT1[30],

likely due to an effect of DGAT1 deficiency in the central nervous system. As this

study has shown no protection from insulin resistance in rats with a liver specific

deficiency in DGAT1, the improvement in insulin sensitivity demonstrated in

previous studies is probably due to weight loss secondary to increased activity.

The important role of DGAT2 in hepatic triglyceride synthesis and the pathogenesis

of insulin resistance has been explored in this study. It is well known that under high

fat feeding conditions, the triglyceride synthesis pathway is activated, and the enzyme

activities of the metabolic intermediates, including DGAT, are increased. In rats

treated with the DGAT2 ASO, the final step—acylation of diacylglycerol to form

triacylglycerol—cannot be completed, and thus triglyceride accumulation is

prevented. As several studies have linked the accumulation of triglycerides in liver

with the pathogenesis of insulin resistance[20,31], it can be suggested that the

improvement in insulin sensitivity demonstrated in this study is likely linked to the

reduction in hepatic triglyceride content also observed.

Complicating this hypothesis, however, is the assumed byproduct of reduced DGAT2

activity—the accumulation of diacylgycerol or another intermediate product of

triglyceride synthesis (Figure 1). Previous studies have linked the accumulation of

these metabolities, especially diacylglycerol, to insulin resistance[32]. It has been

shown that diacylglycerol activates several PKC isomers, which in turn induces

serine/threonine phosporylation of the insulin receptor. This blocks tyrosine kinase

activity on the insulin receptor, which induces insulin resistance[10,20].

Interestingly, analysis of hepatocytes in the rats in the current study revealed no increased accumulation of diacylglycerol or Acyl CoA species (Figure 8). This data, while resolving the conflict with previous data, suggests that an alternate metabolic pathway is activated in these rats to reduce fatty metabolite accumulation. In-vitro data in rat hepatocytes treated with the DGAT2 ASO suggests a shift in the primary function of the cell from lipid synthesis to fatty acid oxidation[33] (Figure 9). In other models involving specific deficiency of the mediators of lipid synthesis, similar data has been found. Knockout of Stearoyl-CoA desaturase, the rate limiting step in monosaturated fatty acid synthesis, increases fatty acid oxidation, likely through a pathway involving AMPK inactivation of Acetyl CoA carboxylase and downstream effects on Malonyl CoA[34]. Other models with increased fatty acid oxidation use different intermediates, including peroxisome proliferators-activated receptor (PPARα) and SREBP1c. The specific mediators involved in the DGAT2 deficient model are as yet undetermined. However, the use of the antisense oligonucleotide may provide the tools necessary to identify the key pathways utilized in this process. In summary, rats with pharmacologically induced deficiency in DGAT2 have less hepatic steatosis and are protected from insulin resistance under high fat feeding conditions. In addition, our results suggest that the deficiency in DGAT2 shifts the primary pathway of lipid in the liver from synthesis to oxidation. Use of the antisense oligonucleotide in this study has provided the unique opportunity to study the metabolic role of DGAT2 in the liver and adipose tissue separate from developmental effects associated with the whole-body knockout model. Equally important, however,

is the potential for DGAT2 as a potential therapeutic target for reduction of hepatic steatosis and insulin resistance in type 2 diabetes.

CITATIONS

1) www.diabetes.org/info/diabetesinfo.jsp

2) Lillioja S, Mott DM, Howard BV, Bennett PH, Yki-Jarvinen H, Freymond D, Nyomba BL, Zurlo F, Swinburn B, Bogardus C. Impaired glucose tolerance as a disorder of insulin action. Longitudinal and cross-sectional studies in Pima Indians. N Engl J Med. 1988 May 12;318(19):1217-25.

3) Lillioja S, Mott DM, Spraul M, Ferraro R, Foley JE, Ravussin E, Knowler WC, Bennett PH, Bogardus C. Insulin resistance and insulin secretory dysfunction as precursors of non-insulin-dependent diabetes mellitus. Prospective studies of Pima Indians. N Engl J Med. 1993 Dec 30;329(27):1988-92.

4) DeFronzo, RA. Pathogenesis of type 2 (non-insulin dependent) diabetes mellitus: a balanced overview. Diabetologia. 1992 Apr;35(4):389-97.

5) Shulman GI. Cellular Mechanisms of Insulin Resistance. J Clin Invest. 2000. 106,171-176.

6) Pan DA, Lillioja S, Kriketos AD, Milner MR, Baur LA, Bogardus C, Jenkins AB, et al. Skeletal muscle triglyceride levels are inversely related to insulin action. Diabetes 1997; 46:1768-1774.

7) Krssak, M. Falk Petersen, K. Dresner, A. DiPietro, L. Vogel, S.M. Rothman, D.L. Roden, M. and Shulman GI. Intramyocellular Lipid Concentrations are correlated with Insulin Sensitivity in Humans: A ^{1}H NMR Spectroscopic Study. Diabetologia. 1999. 42, 113-116.

8) Perseghin G, Scifo P, De Cobelli F, Pagliato E, Battezzati A, Arcelloni C, Vanzulli A, Testolin G, Pozza G, Del Maschio A, Luzi L. Intramyocellular triglyceride content is a determinant of in vivo insulin resistance in humans: a 1H-13C nuclear magnetic resonance spectroscopy assessment in offspring of type 2 diabetic parents. Diabetes. 1999 Aug;48(8):1600-6.

9) Kim JK, Michael MD, Previs SF, Peroni OD, Mauvais-Jarvis F, Neschen S, Kahn BB, Kahn CR, Shulman GI. Redistribution of substrates to adipose tissue promotes obesity in mice with selective insulin resistance in muscle. J Clin Invest. 2000 Jun;105(12):1791-7.

10) Yu C, Chen Y, Cline CW, Zhang D, Zong H, Wang Y, Bergeron R, Jim JK, Cushman SW, Cooney GJ, Atcheson B, White MF, Kraegan EW, and Shulman GI. Mechanism by which fatty acids inhibit insulin activation of insulin receptor substrate-1 (IRS-1)-associated phosphatidylinositol 3-kinase activity in muscle. J Biol Chem. 2002. 277; 50230-50236.

11)   Itani SI, Ruderman NB, Schmieder F, Boden G. Lipid-induced insulin resistance in human muscle is associated with changes in diacylglycerol, protein kinase C, and IkappaB-alpha. Diabetes. 2002 Jul;51(7):2005-11.

12)   Yuan M, Konstantopoulos N, Lee J, Hansen L, Li ZW, Karin M, Shoelson SE. Reversal of obesity- and diet-induced insulin resistance with salicylates or targeted disruption of Ikkbeta. Science. 2001 Aug 31;293(5535):1673-7. Erratum in: Science 2002 Jan 11;295(5553):277.

13)   Hotamisligil GS, Peraldi P, Budavari A, Ellis R, White MF, Spiegelman BM. IRS-1-mediated inhibition of insulin receptor tyrosine kinase activity in TNF-alpha- and obesity-induced insulin resistance. Science. 1996 Feb 2 ;271(5249):665-8.

14)   Shulman GI. Unraveling the cellular mechanism of insulin resistance in humans: new insights from magnetic resonance spectroscopy. Physiology (Bethesda). 2004 Aug;19:183-90.

15)   Cases S, Smith SJ, Zheng YW, Myers HM, Lear SR, Sande E, Novak S, et. al. Identification of a gene encoding an acyl CoA:diacylglycerol acyltransferase, a key enzyme in triacylglycerol synthesis. Proc Natl Acd Sci USA 1998; 95:12018-13023.

16)   Smith SJ, Cases S, Jensen DR, Chen HC, Sande E, Tow B, Sanan DA, et al. Obesity resistance and multiple mechanisms of triglyceride synthesis in mice lacking DGAT. Nat Genet 2000;25:87-90.

17)   Chen, HC, Smith SJ, Ladha Z, Jensen DR, Ferreira LD, Pulawa LK, McGuire JG, et. al. Increased Insulin and Leptin sensitivity in mice lacking acyl CoA:diacylglycerol acyltransferase 1. J Clin Invest 2002; 109:1049-1055.

18)   Stone SJ, Myers HM, Watkins SM, Brown BE, Feingold KR, Elias PM, and Farese RV Jr. Lipopenia and skin barrier abnormalities in DGAT2-deficient mice. J Biol Chem. 2004. 279;11767-11776.

19)   Dean NM, Butler M, Monia BP, Manoharan M: Pharmacology of 2'-O-(2-methyloxy)ethyl-modified antisense oligonucleotide. In: Crooke ST, ed. Antisense Drug Technology: Principles, Strategies and Applications. New York, NY: Dekker 2001; 319-338.

20)   Samuel VT, Liu ZX, Qu X, Elder BD, Bilz S, Befroy D, Romanelli AJ, and Shulman GI. Mechanism of hepatic insulin resistance in non-alcoholic fatty liver disease. J Biol Chem. 2004. 279, 32345-32353.

21) Baker BF, Condon TP, Koller E, McKay RA, Siwkowski AM, Vickers TA, Monia BP. Discovery and analysis of antisense oligonucleotide activity in cell culture. Methods. 2001 Feb;23(2):191-8.

22) McKay RA. Miraglia LJ. Cummins LL. Owens SR. Sasmor H. Dean NM. Characterization of a potent and specific class of antisense oligonucleotide inhibitor of human protein kinase C-alpha expression. Journal of Biological Chemistry. January 1999. 274(3):1715-22.

23) Youn JH, Buchanan TA. Fasting does not impair insulin-stimulated glucose uptake but alters intracellular glucose metabolism in conscious rats. Diabetes. 1993 May;42(5):757-63.

24) Rossetti L, Giaccari A. Relative contribution of glycogen synthesis and glycolysis to insulin-mediated glucose uptake. A dose-response euglycemic clamp study in normal and diabetic rats. J Clin Invest. 1990 Jun;85(6):1785-92.

25) Oshima K, Shargill NS, Chan TM, and Bray GA. Adrenalectomy reverses insulin resistance in muscle from obese (ob/ob) mice. Am J Physiol. 246, E193-E197.

26) Bligh EG, Dyer WJ. A rapid method of total lipid extraction and purification. Can J Biochem Physiol. 1959 Aug;37(8):911-7.

27) Neschen S, Moore I, Regittnig W, Yu CL, Wang Y, Pypaert M, Petersen KF, Shulman GI. Contrasting effects of fish oil and safflower oil on hepatic peroxisomal and tissue lipid content. Am J Physiol. Endocrinol Metab. 2002. 282;E395-E401.

28) Yu XX, Drackley JK, Odle J. Rates of mitochondrial and peroxisomal beta-oxidation of palmitate change during postnatal development and food deprivation in liver, kidney, and heart of pigs. J Nutr 1997; 127:1814-1821.

29) Jandacek RJ, Heubi JE, and Tso P. A novel, noninvasive method for the measurement of intestinal fat absorption. Gastroenterology. 2004. 127;139-144.

30) Smith SJ, Cases S, Jensen DR, Chen HC, Sande E, Tow B, Sanan DA, et al. Obesity resistance and multiple mechanisms of triglyceride synthesis in mice lacking DGAT. Nat Genet 2000;25:87-90.

31) Griffen ME, Marcucci MJ, Cline GW, Bell K, Barucci N, Lee D, Goodyear LJ< Kraegen EW, White MF, and Shulman GI. Free fatty acid-induced insulin resistance is associated with activation of protein kinase C theta and alterations in the insulin signaling cascade. Diabetes. 1999. 48; 1270-1274.

32)   Neschen S, Morino K, Hammond LE, Zhang D, Liu ZX, Romanelli AJ, Cline GW, Pongratz RL, Zhang XM, Choi CS, Coleman RA, Shulman GI. Prevention of hepatic steatosis and hepatic insulin resistance in mitochondrial acyl-CoA:glycerol-sn-3-phosphate acyltransferase 1 knockout mice. Cell Metab. 2005 Jul;2(1):55-65.

33)   Yu XX, Murray SF, Pandey SK, Booten SL, Bao D, Song XZ, Kelly S, Chen S, McKay R, Monia BP, Bhanot S. Antisense oligonucleotide reduction of DGAT2 expression improves hepatic steatosis and hyperlipidemia in obese mice. Hepatology. 2005 Aug;42(2):362-71.

34)   Dobrzyn P, Dobryzn A, Miyazaki M, Cohen P, Asilmaz E, Hardie DG, Friedman JM, and Ntambi JM. Stearoyl-CoA desaturase 1 deficiency increases fatty acid oxidation by activating AMP-activated protein kinase in liver. PNAS 2004. 101;6409-6414.

35)   Savage DB, Petersen KF, Shulman GI. Mechanisms of insulin resistance in humans and possible links with Inflammation. Hypertension. 2005 May; 45(5):828-33.

FIGURES
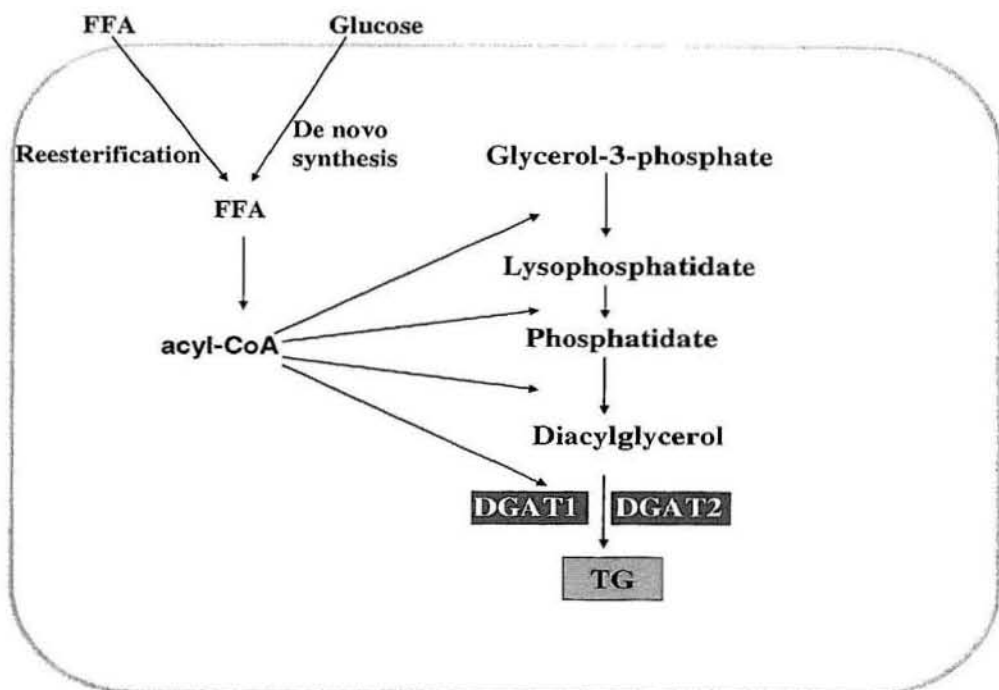
Figure 1. Trigylceride Synthesis Pathway

The two isoforms of Diacylglycerol Acyltransferase (DGAT1 and DGAT2) catalyze

the final step in both the de-novo and re-esterification pathways leading to

triglyceride synthesis. Prior to addition of an acyl-CoA group to diacylglyerol to

form triacylglycerol, several other enzymes, including Acyl-CoA:glycerol-sn-3-

phosphate acyltransferase (GPAT), acyl-CoA:1-acylglycerol-sn-3-phosphate

acyltransferase (AGPAT) and phosphatidic acid phosphatase (PAP) sequentially add

acyl-CoA groups to several intermediates, beginning with Glycerol-3-phosphate.

Glycerol 3 phosphate is generated de-novo or via re-esterification of the products of

fatty acid oxidation.

DGAT 1& 2 Gene Expression in Liver
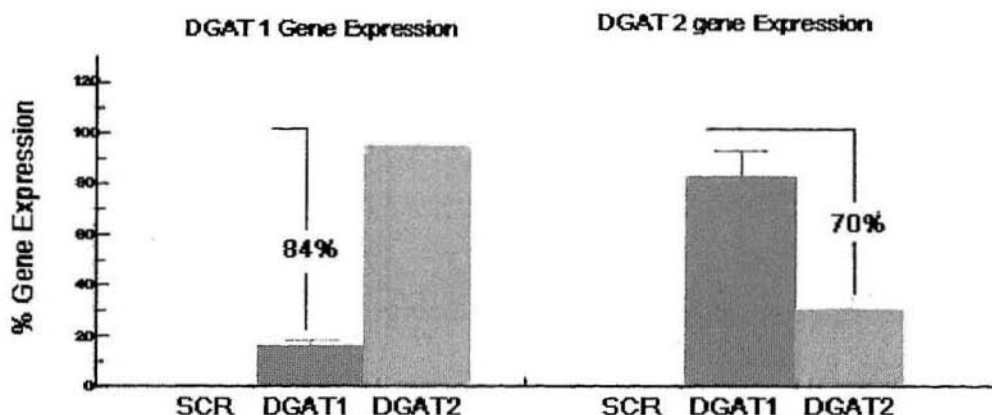
Figure 2. DGAT1 and DGAT2 Gene expression after ASO treatment

WT animals were treated with a nonsense (scrambled), DGAT1, or DGAT2 ASO for

four weeks while on a high-fat diet (SCR=Scrambled ASO, DGAT1=DGAT1 ASO

Treatment, DGAT2=DGAT2 ASO Treatment). Baseline values of gene expression

were measured in a separate group prior to treatment. Gene expression was measured

in rats receiving four weeks of treatment. Livers were collected under fasting

conditions using an in-situ freeze-clamp technique. Values expressed as percent

suppression from baseline + SEM.
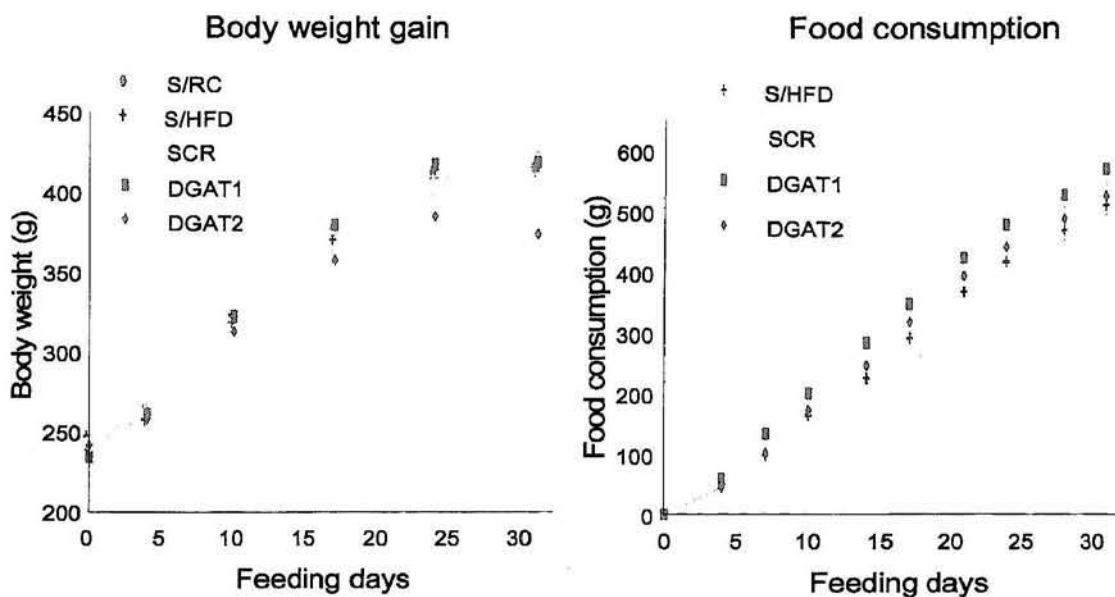
Figure 3. Body Weight Gain and Food Consumption during treatment period.

Body weight and food consumption was measured biweekly immediately prior to

treatment in all treatment groups—Saline treatment on regular chow (S/RC), Saline

treatment on high fat diet (S/HFD), Scrambled ASO treatment on high fat diet (SCR),

DGAT1 ASO treatment on high fat diet (DGAT1), and DGAT2 ASO treatment on

high fat diet (DGAT2)—over the four week treatment period. Results are expressed

in grams.
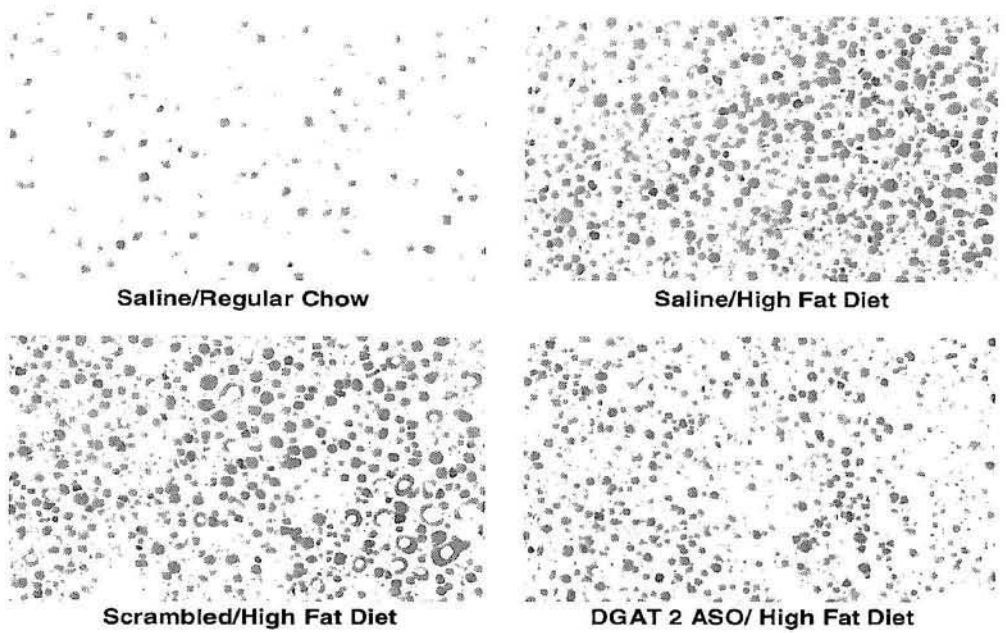
Figure 4. Histologic Analysis of Hepatocytes

Representative histology of rat hepatocytes after four weeks of either Saline treatment

on regular chow, Saline treatment on a high fat diet, Scrambled ASO treatment on a

high fat diet, or DGAT2 ASO treatment on a high fat diet.
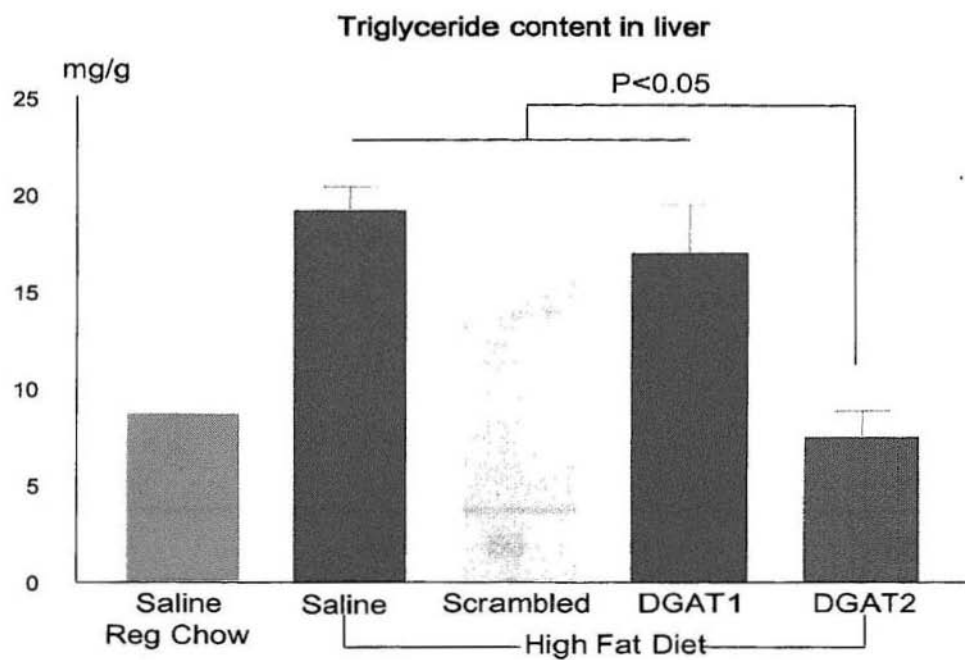
Figure 5. Triglyceride Content in Liver

Liver triglyceride content was measured in all five groups at the end of the four week

treatment period. Rats were given regular chow or a high fat diet and treated with

saline, nonsense (scrambled) ASO, DGAT1 ASO, or DGAT2 ASO. Livers were

obtained via in-situ freeze clamping after overnight fast. Results are expressed as

mean triglyceride content (in milligrams per gram of liver) + SEM.

Figure 5. Triglyceride Content in Liver

Liver triglyceride content was measured in all five groups at the end of the four week treatment period. Rats were given regular chow or a high fat diet and treated with saline, nonsense (scrambled) ASO, DGAT1 ASO, or DGAT2 ASO. Livers were obtained via in-situ freeze clamping after overnight fast. Results are expressed as mean triglyceride content (in milligrams per gram of liver) + SEM.

6A: Glucose Infusion Rate (GINF) during clamp period
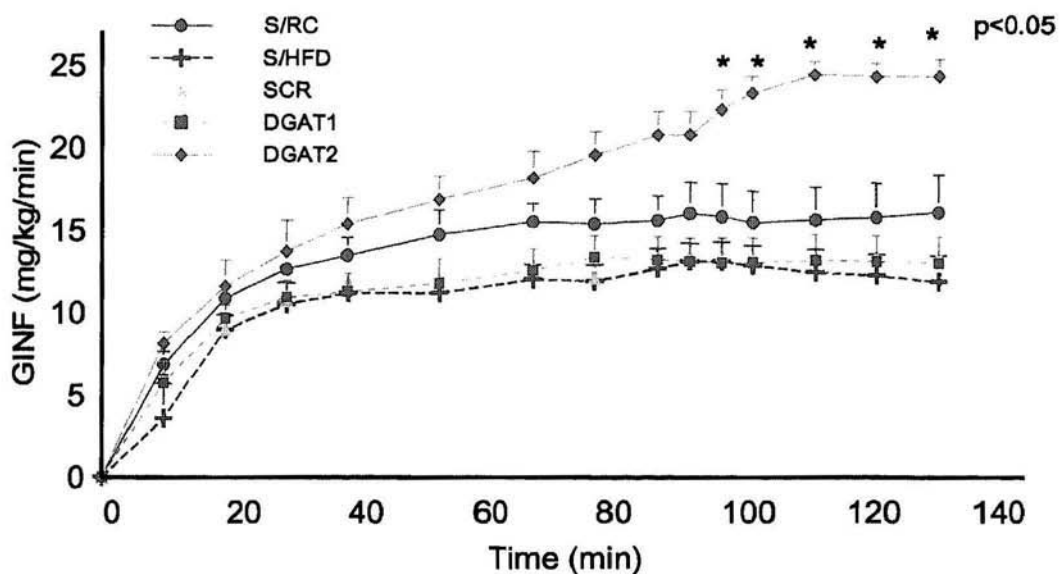
6B: Insulin Mediated Suppression of Hepatic Glucose Production

6A: Glucose Infusion Rate (GINF) during clamp period

6B: Insulin Mediated Suppression of Hepatic Glucose Production

6C: Insulin Mediated Effect on Glucose Uptake, Glycolysis, Glycogen Synthesis
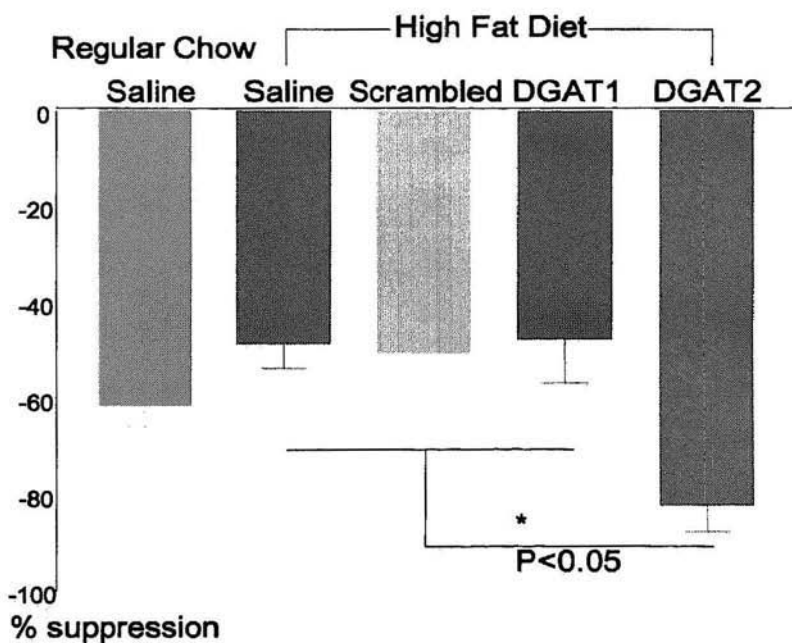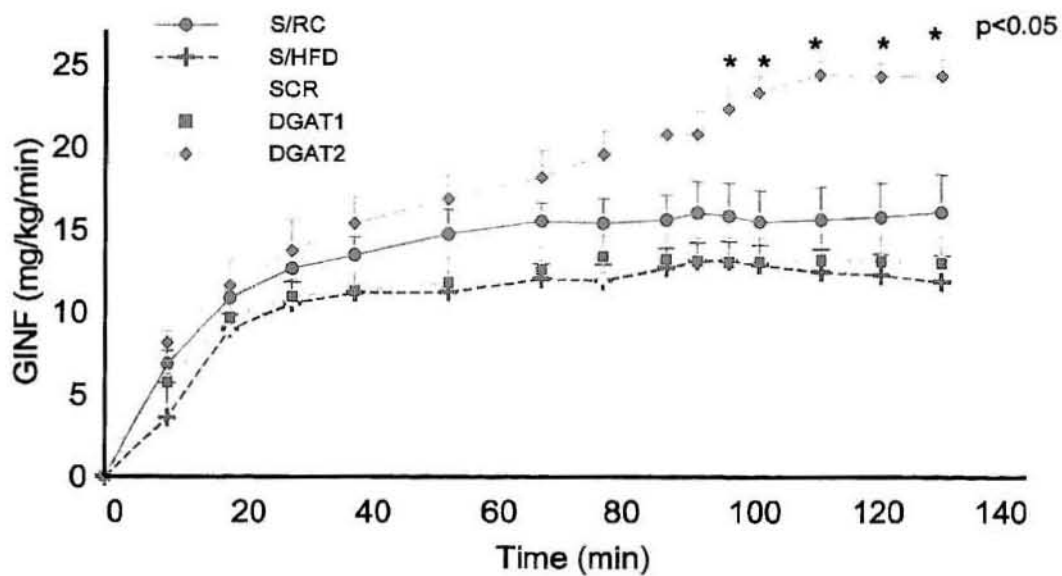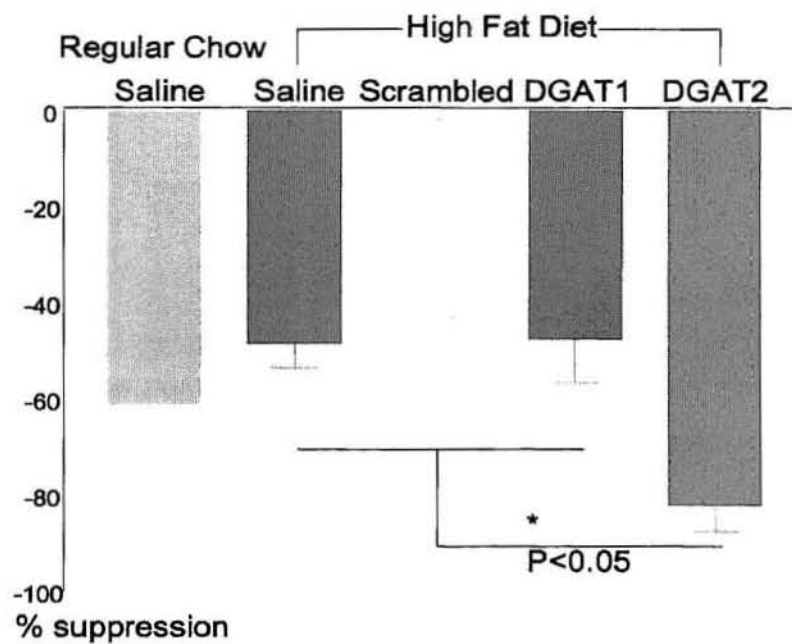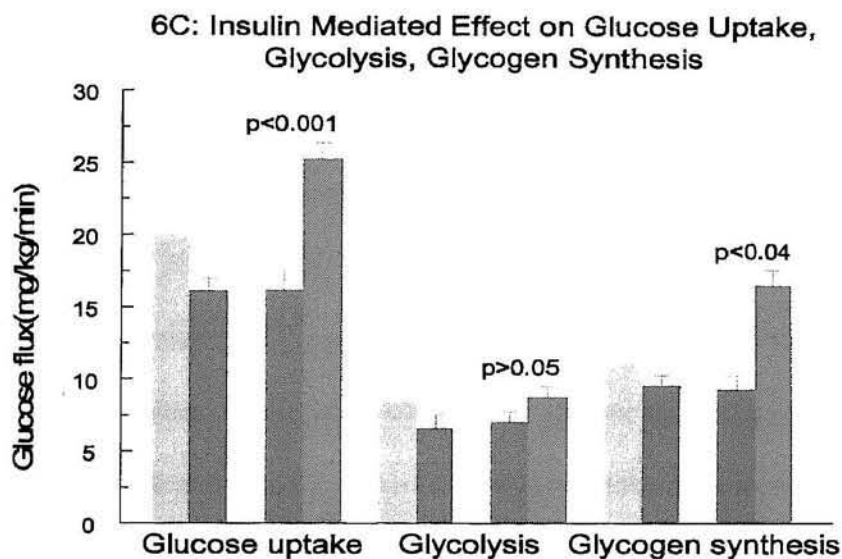
6D: Glucose uptake: Soleus
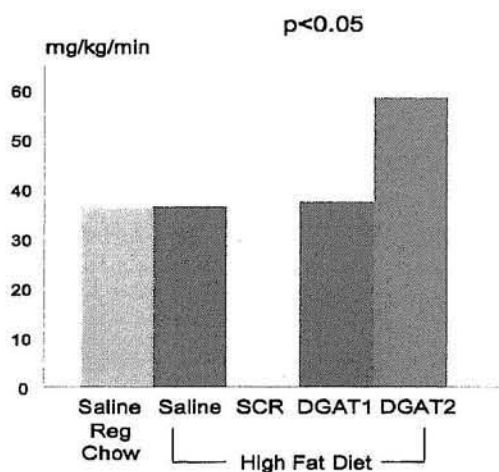
6E: Glucose uptake: Adipose
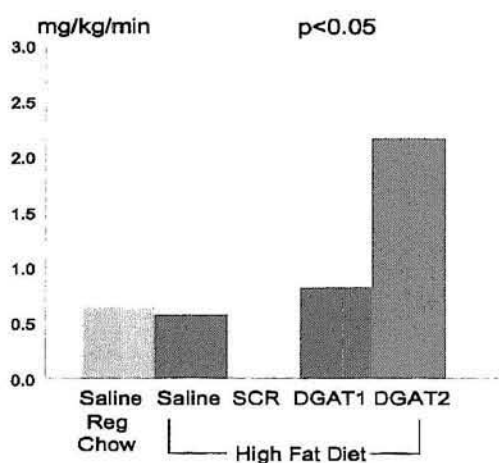
Figure 6. Hyperinsulinemic-Euglycemic Clamp Experiments

Wild-type rats were separated in into five treatment groups: Saline treatment in rats

receiving regular chow (S/RC; n=7), saline treatment in rats receiving a high fat diet

(S/HF; n=7), and high fat fed rats receiving treatment with either a nonsense ASO (SCR; n=14), DGAT1 ASO (DGAT1; n=11), or DGAT2 ASO (DGAT2; n=9). After a 14 hour fast, all treatment groups underwent hyperinsulinemic-euglycemic (4 mU/kg/min) clamp experiments. Plasma glucose was maintained by variable intravenous infusion of 20% glucose, as recorded (A). Once steady state conditions were achieved, insulin-mediated suppression of hepatic glucose production was determined (B). In addition, steady state whole body glucose uptake, glycolysis, and glycogen synthesis were measured(C). Individual tissue uptake of glucose in skeletal muscle (D) and adipose tissue (E) was determined using the ^{3}H radioactive marker. All values are expressed as means ± SEM.
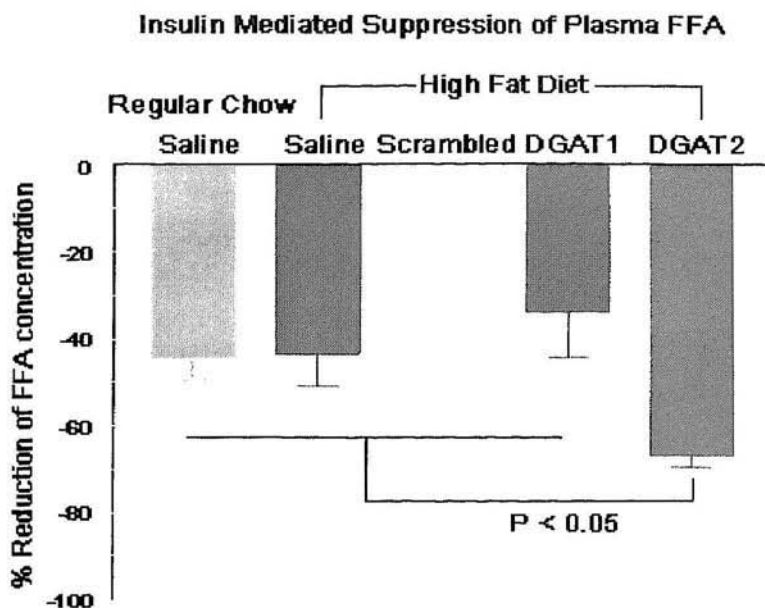
Figure 7. Insulin effect on plasma free fatty acid concentration.

In all five experimental groups, after the treatment period and an overnight fast,

plasma was drawn at baseline (time = 0) and again at 185 minutes after insulin

stimulation (during the hyperinsulinemic-euglycemic clamp) to measure insulin

stimulated suppression of plasma free fatty acid concentration. Results are expressed
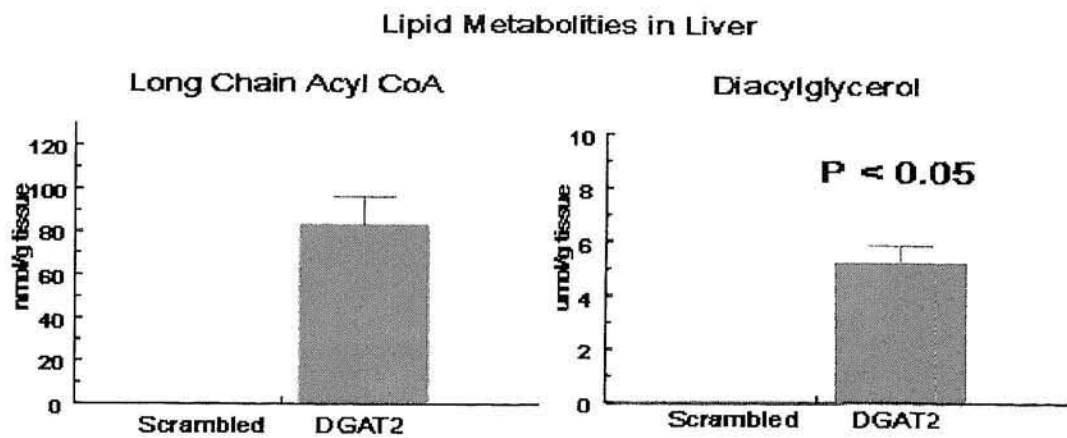
as mean percentage suppression + SEM.

Lipid Metabolites in Liver

Figure 8. Measurement of lipid metabolites

After a 14 hour fast, Long chain acyl-CoA (A) and diacylglycerol (B) species were

extracted from the livers of rats from the nonsense and DGAT2 ASO treatment

groups. An API 3000 tandem mass spectrometer interfaced with a turbo ionspray

source in negative electrospray mode measured individual species. Values shown are
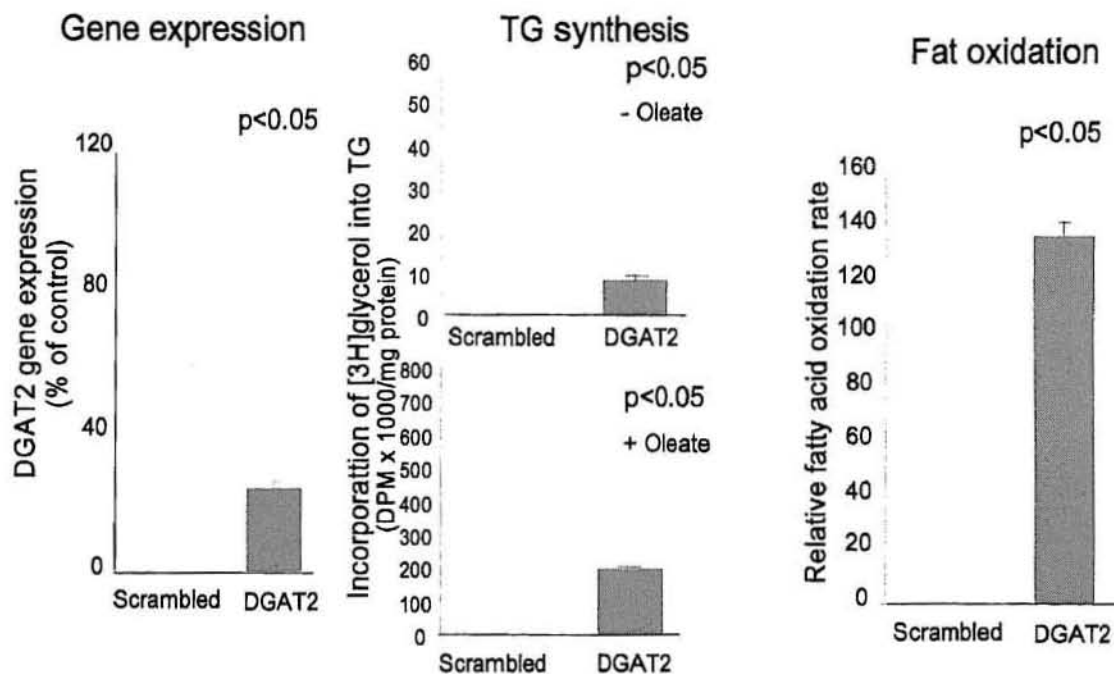
means + SEM.

Figure 9. Effect of DGAT2 ASO on triglyceride synthesis and fat oxidation in cultured rat hepatocytes.

Rat hepatocytes were transfected with either a nonsense or DGAT2 ASO. Once it was determined that gene expression was suppressed (A), trigylceride synthesis in transfected rat hepatocytes was determined by measuring the incorporation of radiolabeled glycerol into triglycerides with and without oleate (B), a crucial compound for de novo synthesis. Fat oxidation was then measured (C). All values in mean + SEM.
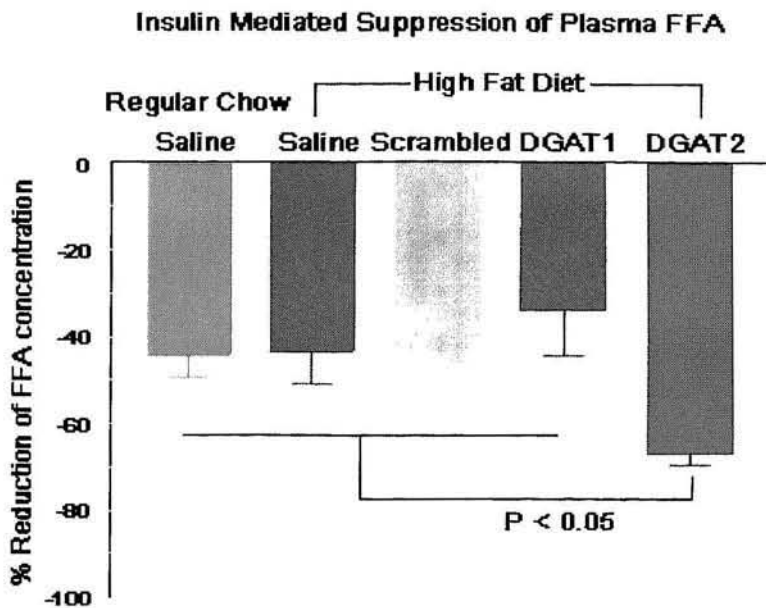
Figure 7. Insulin effect on plasma free fatty acid concentration.

In all five experimental groups, after the treatment period and an overnight fast,

plasma was drawn at baseline (time = 0) and again at 185 minutes after insulin

stimulation (during the hyperinsulinemic-euglycemic clamp) to measure insulin

stimulated suppression of plasma free fatty acid concentration. Results are expressed
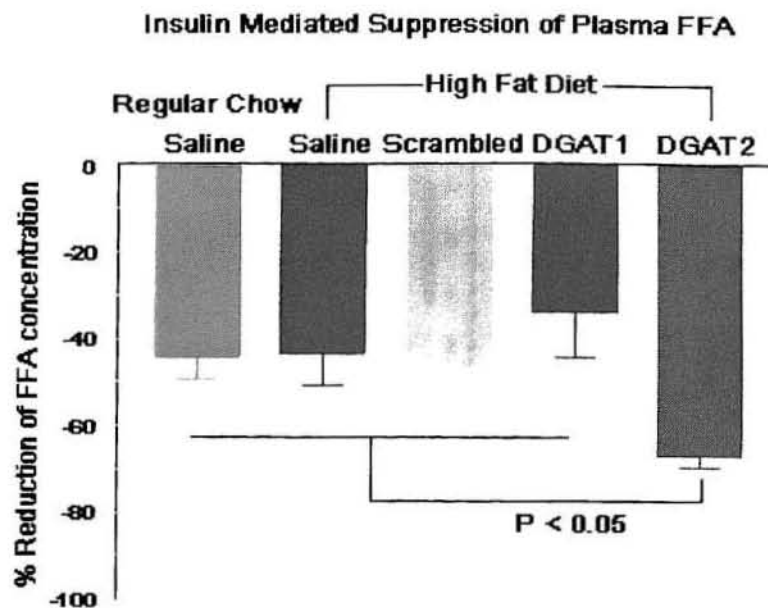
as mean percentage suppression + SEM.

Figure 7. Insulin effect on plasma free fatty acid concentration.

In all five experimental groups, after the treatment period and an overnight fast,

plasma was drawn at baseline (time = 0) and again at 185 minutes after insulin

stimulation (during the hyperinsulinemic-euglycemic clamp) to measure insulin

stimulated suppression of plasma free fatty acid concentration. Results are expressed
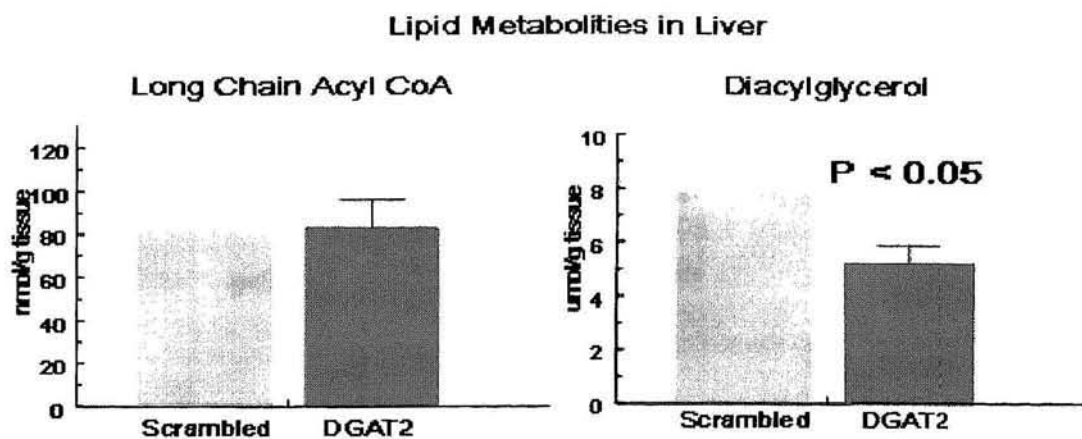
as mean percentage suppression + SEM.

Lipid Metabolities in Liver

Long Chain Acyl CoA

Diacylglycerol

P ≤ 0.05

Figure 8. Measurement of lipid metabolites

After a 14 hour fast, Long chain acyl-CoA (A) and diacylglycerol (B) species were

extracted from the livers of rats from the nonsense and DGAT2 ASO treatment

groups. An API 3000 tandem mass spectrometer interfaced with a turbo ionspray

source in negative electrospray mode measured individual species. Values shown are
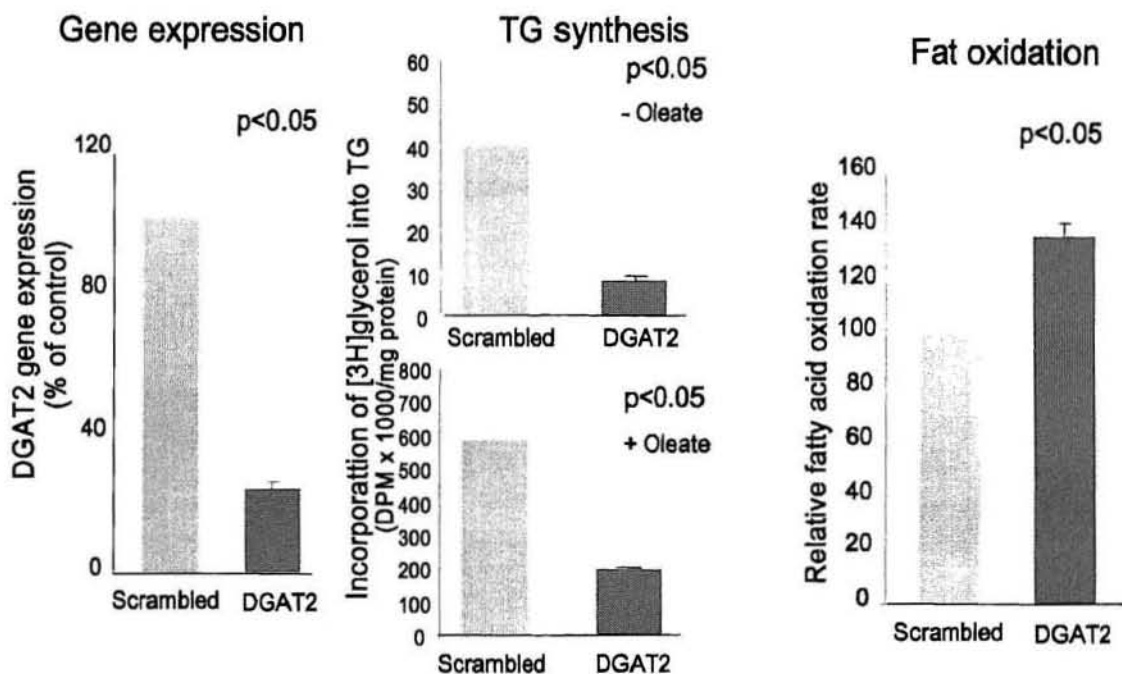
means + SEM.

Figure 9. Effect of DGAT2 ASO on triglyceride synthesis and fat oxidation in cultured rat hepatocytes.

Rat hepatocytes were transfected with either a nonsense or DGAT2 ASO. Once it was determined that gene expression was suppressed (A), trigylceride synthesis in transfected rat hepatocytes was determined by measuring the incorporation of radiolabeled glycerol into triglycerides with and without oleate (B), a crucial compound for de novo synthesis. Fat oxidation was then measured (C). All values in mean + SEM.

HARVEY CUSHING/JOHN HAY WHITNEY MEDICAL LIBRARY

MANUSCRIPT THESES

Unpublished theses submitted for the Master's and Doctor's degrees and deposited in the Medical Library are to be used only with due regard to the rights of the authors. Bibliographical references may be noted, but passages must not be copied without permission of the authors, and without proper credit being given in subsequent written or published work.

This thesis by
has been used by the following person, whose signatures attest their acceptance of the above restrictions.

NAME AND ADDRESS   **DATE**